Proceedings of the 4th International Symposium on the Analysis of

Seismicity and Seismic Risk

Bechyně Castle, Czechoslovakia, September 4-9, 1989

SYNTHESIS OF STRONG GROUND MOTION IN GREECE

G-Akis Tselentis
Laboratory of Theoretical and Applied Seismology
The University of Patras, Patras 261 10, Greece

A B S T R A C T

This paper addresses the problem of strong ground motion synthesis in the area of Greece, by combining probabilistic seismic hazard analysis and stochastic earthquake motion models, together with semi-empirical and theoretical methods of synthesis.

First, a standard probabilistic seismic hazard analysis is applied taking into account the nearby seismogenic zones and the relation between the peak ground motion intensity (e.g. acceleration) and the corresponding annual probability of exceedance is evaluated.

Second, the ground motion parameters such as duration, predominant frequency and spectral shape are expresses as functions of earthquake magnitude and distance and are determined as conditional means corresponding to the annual probability of exceedance for the ground motion intensity. On this basis, risk consistent earthquake motions are generated using the previously derived parameters.

Third, for the situation that a well known seismogenic fault exists near the site under consideration, the body wave of the expected ground motion is synthesized by utilizing small synthesized earthquakes as Green's functions. These elementary earthquakes in the case of small recorded motions are estimated using Brune's spectrum for each subfault. On the other hand, the long period ground motion is synthesized by employing fault dislocation and normal mode theories.

Finally, some characteristic examples from three sites in Greece are presented.

1. INTRODUCTION

In order to prevent and mitigate earthquake disasters, it is necessary to assess hazards caused by future earthquakes. An estimation of strong ground motion is important for the hazard assessment. In designing a structure to withstand the effects of strong earthquake ground motions, it is necessary to characterize the type of motion to which that structure is likely to be subjected.

In general earthquake ground motions are mainly governed by the three factors: source mechanism, propagation path of earthquake waves and local soil layers around the structures. The significant estimate of earthquake ground motions, therefore, should deal with the three factors in a well-balanced manner, since these motions are caused by their overall effect.

While both engineers and seismologists recognize the stochastic nature of high-frequency ground motions (Boore 1983), they estimate them in fundamentally different ways. The engineer relies heavily on an empirical approach in which the motions are constructed so as to agree in essential ways (e.g. amplitude, frequency content and duration) with existing data, and various techniques for synthesis have been proposed, ranging from filtering and windowing Gaussian noise to adding

together suitably scaled recorded accelerograms.

The seismologists on the other hand rely on more physical models. These models usually involve the prediction of the motions from a fault with known dimensions and rupture parameters.

There are many ways to generate an accelerogarm on a digital computer to represent the ground motion expected at a site at a certain distance from a potential earthquake source. In the future, it may come a time when enough recorded accelerograms become available and the need for artificial accelerograms in seismic design and analysis will gradually decrease. At present time simulated earthquake ground motions still serve a very useful purpose.

It is essential to develop a prediction model for earthquake ground motions corresponding to a particular structural system, based on the available seismological data. The greater the importance of the structure the more data necessary for the prediction of adequate input earthquake motions. Therefore, earthquake motions are also required at sites where little data are available. In those cases, the seismologist should provide a reliable earthquake motion that can be used for the safe design of the structures at that sites. This means that the earthquake motions adequate to important structures may be generated by rigorous algorithms based on accurate seismotectonic or geological data, but those corresponding to conventional ones should be estimated by simple methods considering earthquake parameters, such as earthquake magnitude and source to site distance, that can be easily obtained.

The purpose of the present paper is to describe briefly the procedure used by the laboratory of Theoretical and Applied Seismology of Patra's University in order to assess the expected strong ground motion at sites whose tectonic setting and local soil conditions are known.

2. FIRST STAGE: SIMULATION OF RISK CONSISTED EARTHAQUAKE MOTION

During this stage, the ground motion intensity parameter is first determined using the conventional hazard curve technique. Then the procedure developed by Kameda and Nojima (1988) is followed and the other parameters such as duration, predominant frequency and spectral shape are determined as conditional means corresponding to a set of earthquakes limited from the probability of exceedance for the intensity parameter.

Thus, the probability of exceedance for the intensity parameter is the only index to be specified and all the required for the ground motion synthesis parameters can be determined probabilistically.

2.1 Evaluation of the intensity parameter from the hazard curve.

Earthquake motion intensity is represented by the peak RMS acceleration γ_0. The value $\gamma = \gamma_0$ corresponding to the annual probability of exceedance Po is determined by employing conventional seismic hazard techniques, i.e.,

$$p_0 = 1 - \exp\left[-\sum_{k=1}^{l} \nu_k A_k q_k(\gamma_0)\right] \cong \sum_{k=1}^{l} \nu_k A_k q_k(\gamma_0) \qquad 1$$

Suppose that there are l potential earthquake sources in the region of a site. Also suppose that k is the average occurrence rate of earthquake with the upper and lower boundary magnitude m_{uk} and m_{lk}, and Ak is the area in source k. $q_k(\gamma_0)$ represents the probability that the random intensity exceed γ_0 at the site on condition that an earthquake occurs somewhere in source k, and my be given as follows.

$$q_k(\gamma_0) = \int_{m_{lk}}^{m_{uk}} \int_{r_{lk}}^{r_{uk}} P\left[U > \frac{\gamma_0}{\gamma(m,r)}\right] f_{Rk}(r) f_{Hk}(m)\, dr\, dm \qquad 2$$

where $f_{Mk}(m)$ is the probability density function of magnitude M in source k, $f_{Rk}(r)$ is the probability density function of epicentral distance R (upper and lower value r_{uk}, r_{lk}) in source k, $\gamma(m,r)$ is the attenuation equation for represented by Eq.[5], U is the lognormal variate representing attenuation uncertainty with median of 1.0 and coefficient of variation δ_γ. Kameda and Sugito (1982), proposed $\delta_\gamma = 0.427$ as the level of uncertainty of intensity parameter considering site information.

Hazard curve is obtained by calculating Po from Eq.[1] for many values of and the value δ_γ which corresponds to an arbitrary value of Po can be read directly from this hazard curve.

2.2 Evaluation of other ground motion parameters as conditional mean.

Given the value γ_0 for a prescribed value of Po, then other ground motion parameters are estimated as conditional mean values given that $\Gamma > \gamma_0$. The concept is illustrated schematically in Fig.1, showing the conditional probability of $\Gamma > \gamma_0(Po)$ for given values of magnitude and distance, m and r, respectively. Obviously, when $\sigma_\gamma = 0$, one can draw a definite border line in Fig.1 dividing the area where $P(\Gamma > \gamma_0(Po) | m,r) = 1$ and that where $P(\Gamma > \gamma_0(Po) | m,r) = 0$. On this account, the model parameters (except γ typically denoted by b are determined from

$$\bar{b}(Po) = E[b | \Gamma > \gamma_0(Po)] \qquad 3$$

where the probability $P(\Gamma > \gamma_0(Po) | m,r)$ takes the role of a weighting function in determination of the conditional mean.

In this way, all of the model parameters can be determined from a single index Po and one can avoid using complex multi-dimensional probability distribution. Thus, the conditional mean of b corresponding to given Po is calculated from

$$\bar{b}(p_0) = \sum_{k=1}^{l} \nu_k A_k \bar{b}_k(p_0) \;/\; \sum_{k=1}^{l} \nu_k A_k \qquad 4$$

where $\bar{b}$ (Po) is the conditional mean of b in source k, given Po and it can be expressed (Kameda and Nojima 1988) as

$$\bar{b}_k(p_0) = \frac{1}{q_k(\gamma_0)} \int_{m_{lk}}^{m_{uk}} \int_{r_{lk}}^{r_{uk}} a(m,r) P\left[U > \frac{\gamma_0}{\gamma(m,r)}\right] f_{Rk}(r) f_{Mk}(m)\, dr\, dm \qquad 5$$

2.3 Ground motion estimation model

An earthquake acceleration ground motion record a(t) can be represented as follows

$$\alpha(t) = \sum_{k=1}^{m} \sqrt{2G(t,\omega_k)\Delta\omega} \cdot \cos(\omega_k t + \phi_k) \qquad 6$$

in which $G(t,\omega_k)$ is the evolutionary spectrum for time t and angular frequency ω_k, ϕ_k is an independent random phase angle taking values between 0 and 2π, and m is the number of superposed harmonic components. We have adopted the Evolutionary Process Model proposed by Sugito and Kameda (1985) for the prediction of earthquake motion on baserock, known as EMP-IBR model. The evolutionary spectrum according to the above model can be expressed as

$$G(t,2\pi f) = \alpha_f(t) \frac{2\beta_g(t)}{\pi^2 f_p(t)} \cdot \frac{[f/f_p(t)]^2}{\{1-[f/f_p(t)]^2\}^2 + 4\beta_g^2(t)[f/f_p(t)]^2} \qquad 7$$

in which $a_f(t)$ is the intensity parameter which represents mean square intensity at time t, $f_p(t)$ is the predominant frequency at time t and $\beta_g(t)$ is the spectral shape parameter at time t. These parameters can be expressed as the time dependent functions

$$\alpha_f(t) = \gamma^2 (t/t_m)^2 \exp\{2(1-t/t_m)\}$$
$$f_p(t) = f_{p0} + A_1(t - t_m) \quad , \quad \beta_g(t) = \beta_{g0} + B_1(t - t_m) \qquad 8$$

where t_m is the time for maximum value of $a_f(t)$ and $\gamma = a_f(t_m)$ is the peak RMS intensity. f_{p0}, β_{g0}, A1, B1 are parameters which are independent of time. The regression equations listed in Table 1 (Sugito and Kameda 1985) establish the prediction model for given magnitude and epicentral distance).

2.4 Application for the city of Corinth

A data base of earthquake records with magnitudes greater than 5 corresponding to the area of Greece was prepared taking into account the catalogs of Makropoulos and Burton (1981) and Comninakis and Papazachos (1986). In the analysis the area source model was chosen to represent seismic source zones around the site. The region of Greece was divided into the 19 seismic zones proposed by Papazachos (1980), on the basis of seismotectonic criteria (Fig.2).

Fig.3, shows the obtained hazard curve which corresponds to the city of Corinth, for various values of σ_γ. In this study, analysis has been developed comparing the case $\sigma_\gamma = 0.427$ with the case $\sigma_\gamma = 0.0$.

Fig.4, shows the estimated values of t_m(Po), f_{p0}(Po), β_{g0}(Po). With the technique mentioned previously, simulated ground motions can be generated for given Po.

In Fig.5, we show the expected (for baserock), ground motion for Po=0.01 (return period 100 years).

3. STAGE 2: SEMI-EMPIRICAL METHOD TO ESTIMATE EXPECTED STRONG GROUND MOTION NEAR A KNOWN FAULT

The method for earthquake motion synthesis presented in the previous paragraph, does not consider the nature of the earthquake source (geometrical characteristics, rupture process) and the effect of propagation path. In the case that near the site under investigation exists a well known seismogenic fault it is necessary, especially for the case of critical structures, to estimate reliable input earthquake motions taking into account the various fault parameters and the propagation characteristics.

First Hartzell (1978), proposed a method to synthesize strong earthquake motions, utilizing observed seismograms from small events as Green's functions. The earthquake motion during the major earthquake was generated by assuming earthquake sources distributed on the fault plane, with source spectra corresponding to those of the closest associated aftershock (Fig.6). The use of aftershocks as Green's functions has the advantage that the complex rupture process on the fault plane, as well as the path effects are incorporated in the modeling process. In Hartzell's method, the discrepancy between the rise time of the large and the small event was not taken into account.

Irikura and Muramatsu (1982) improved Hartzell's method by introducing the phase delayed summation with a specific time function to consider the difference in the source time function between the main shock and the small events. Tanaka et al (1982), pointed out that Irikura and Muramatsu's method overestimates the wave amplitude around 1/Tr, where Tr is the rise time of the elementary earthquake, for frequencies greater than 1/Tr. They proposed a method to simulate an accelerogram by adding the contribution of small event records over the length and the width of the large event's fault.

Dan et al (1986), combined Irikura and Muramatsu's and Tanaka et al.'s method to synthesize the acceleration ground motions for the 1979 Imperial Valley earthquake. They adopted the Irikura and Muramatsu's method in the lower frequency range and Tanaka et al.'s method for the higher frequency range. They simulated well the peak values, duration times and spectral characteristics of the observed motions.

In the present approach, the source spectra for both events are modeled by the far field shear wave displacement spectra (Brune 1970)

$$\Omega(\omega) = F^S \cdot \left(\frac{\lambda}{X}\right) \cdot \left(\frac{\sigma_e}{\mu}\right) \cdot \frac{\beta}{(\omega_c + j\omega)^2} \cdot \left(1 - \frac{2\pi}{Q}\right)^{\omega X/4\pi\beta} \quad 9$$

where F^S is the radiation pattern of the shear wave, λ is the source size, X is the hypocentral distance, σe is the effective stress, μ is the rigidity of the medium, β is the shear wave velocity, ωc is the corner frequency, Q is the quality factor. Note that the corner frequency is given by

$$\omega_c = 2\beta\sqrt{\pi\lambda\sigma_e / M_0}, \quad 10$$

where Mo is the seismic moment.

Considering that $\lambda = (LW/\pi)^{1/2}$ and $Mo = \mu LWD$ (L=rupture fault length, W= fault width, D= average dislocation), and assuming that the ratios of L, W, D, σ of the large event to those of the small event are equal to a, b, c and d, the expected spectrum generated by the [p,q] element whose size is equal to that of the small event is described by

$$\Omega_{pq}(\omega) = \left(\frac{X_s}{X_{pq}}\right) \cdot d \cdot \left(\frac{\omega_{cs} + j\omega}{\omega_{cs}\sqrt{d/c} + j\omega}\right)^2 \cdot \left(1 - \frac{2\pi}{Q}\right)^{\omega(X_{pq} - X_s)/4\pi\beta} \cdot \Omega_s(\omega) \quad 11$$

Thus, the expected motion during the large earthquake can be synthesized as

$$u_l(t) = \sum_{p=1}^{a} \sum_{q=1}^{b} u_{pq}(t - t_{pq}) \quad 12$$

where u_{pq} is the inverse Fourier transform of eq.[11] and t_{pq} is the travel time lag for the rupture process and the wave propagation.

3.1 Application: Synthesis of the 1986 Kalamata earthquake

Details about the Kalamata Sept.13 earthquake can be found in the literature (e.g. Tselentis et. al 1989) and are not documented here. In general, its aftershock distribution was divided into two clusters separated by a gap. The epicenter of the main shock (Ms=6.2), was placed at the Northern cluster and

that for the major aftershock (Ms=5.4),at the southern cluster (Fig.7). For the synthesis we assumed that the rupture corresponds to the Northern cluster only. The parameters which were used for the simulation are listed in Table 2. Considering the similarity relations of Kanamori and Anderson (1975), the ratios of ruptured length, width, average dislocation and effective stress of the main shock to those of the major aftershock were assumed equal to 3,3,3 and 1 respectively. At station NOM (Fig.7), both main shock and aftershock records were available. Using the aftershock records as Green functions, the main shock was synthesized and is compared with the observations in Fig.7. Judging from this figure we conclude that the amplitude, wave form and duration of the strong motion were simulated well.

4. STAGE 3: SYNTHESIS OF EXPECTED LONG PERIODS IN STRONG GROUND MOTION

Aseismic design of structures with long dimensions such as tall buildings, large oil tanks, ech., is usually controlled by large strains and relative displacements induced by surface waves propagating with relatively low horizontal velocities.

For long period ground motions, the contribution of the surface waves may be larger than that of the body waves at large epicentral distances, especially in the case of shallow earthquakes. A number of studies (Herrman and Nuttli 1975, Swanger and Boor 1978, Kudo 1978,80) showed that long period ground motions observed at moderate or long distances were simulated very well by the synthetic surface waves.

4.1 Method of synthesis

During the following synthesis, the target faults are subdivided into kxn rectangular subfault segments. The corresponding field displacement spectra in the radial direction for the [k,n] subfault can be written using the results of normal mode theory (e.g. Ben-Menahem and Singh 1980) as

$$Skn=\sum_{j=1}^{N(w)}\frac{M(w)Vzj(w,z)Xj(w,h,\vartheta)}{2Cj(w)Uj(w)Aj(w)[2\pi rKj(w)]^{1/2}}\cdot \exp[-i(Kj(w)r+3\pi/4)-\gamma jr] \quad 13$$

in which w=angular frequency, N(w)=upper limit of modal superposition at a given frequency, j=number of modes, Kj= wavenumber of the j-th mode, Cj=phase velocity, Uj=group velocity, Qj=quality factor, o=azimuth angle measured anticlockwise from strike, z=depth, h=focal depth for each subfault.

The complex radiation pattern function for the case of Rayleigh waves can be written as

$$X(\vartheta,h)=[\frac{\omega V_R}{c}][0.5(\frac{3\lambda(h)+2\mu(h)}{\lambda(h)+\mu(h)})\sin 2d\sin s- \quad 14$$

$$0.5\sin 2d\sin s\cos 2\vartheta-\sin d\cos s\sin 2\vartheta]+\frac{T_z(h)}{\lambda(h)+2\mu(h)}$$

$$\sin 2d\sin s+i\frac{T_R(h)}{\mu(h)}(\cos d\cos s\cos\vartheta-\cos 2d\sin s\sin\vartheta)$$

and for the case of Love waves as

$$X(\vartheta,h)=[\frac{\omega V_2(h)}{c}](\sin d\cos s\cos 2\vartheta-0.5\sin 2d\sin s\sin 2\vartheta)+$$

$$i\frac{T_2(h)}{\mu(h)}(\cos 2d\sin s\cos\vartheta+\cos d\cos s\sin\vartheta) \quad 15$$

where s=slip angle measured counterclockwise from a horizontal line parallel to the strike, d=dip angle measured downward from the North and Vz,Tz,Vr,Tr are the normal mode solutions.

The parameter Aj(w) in eq.[13] is defined for the case of Love waves as

$$Aj(w)=\int_0^\infty p(z)Vz(z)dz \quad 16$$

and for the case of Rayleigh waves as

$$Aj(w)=\int_0^\infty p(z)[V_z^2(z)+V_r^2(z)]dz \quad 17$$

The vertical component for the case of Rayleigh waves were determined from the radial components by multiplying them with $[Vr(0)/Vz(0)]\exp(-i\pi/2)$

The spectral source time function M(w) is given as the Fourier transform of the source time function $S(t)=\mu SU(t)$ where U(t) is the dislocation time history. For a simple Haskell-type dislocation with a modified ramp function having a rise time r, the spectral source function becomes

$$M(w)=\mu SU[\pi\delta(w)+(2\sin(wr/2)/(iw^2r))\exp(-iwr/2) \quad 18$$

where $\delta(w)$ is Dirac's delta function.

By summing the contribution of each individual subfault, the ground motion is expressed as

$$u(t)=\sum_k\sum_n\int Skn(w)\exp[jw(t-tj)]dw \quad 19$$

where tj is the delay time depending on both the rupture velocity and the propagation wave velocity in the media.

$$tj = [\vec{rj}-\vec{ro}]/Vr + (rj-ro)/Vs \qquad 20$$

Effect of the propagation rupture along the fault length was taken into account for each one subfault separately by multiplying the corresponding spectra by

$$\exp(-iX)\sin X/X$$

where

$$X=0.5wL(L/Vr - \cos\delta/C(w)) \quad (r>>L) \qquad 21$$

assuming a unilateral rupture to strike direction.

4.2 Application: expected surface waves in Athens due to the Atalanti earthquake

The increasing number of high-rise buildings and large scale structures in Athens result in an urgent need to determine the characteristics of strong ground motions for periods greater than 2 sec. A potential large earthquake which is expected to occur in the not too distant future at a major fault located near Athens is considered in the present investigation.

We assume a maximum expected amplitude (Ms) of about 7 and the expected fault length is estimated from the proposed relation between fault length and magnitude for the area of Greece (Kiratzi et al 1985)

$$LogL=0.61Ms-2.55 \qquad 22$$

while the expected fault dislocation (U) was estimated by employing Sato's (1979) empirical formula

$$LogU=0.5Ms-1.4 \qquad 23$$

and the seismic moment is calculated from the following relation proposed for the area of Greece (Tselentis et al 1988)

$$LogMo=1.16Ms+18.9 \qquad 24$$

Geller's (1978) empirical formula was used to estimate the expected rupture velocity

$$Vr=0.72Vs \qquad 25$$

which for a shear wave velocity of 3.86 Km/s results in a rupture velocity of 2.78 Km/s. Of course, assuming a uniform rupture velocity along the fault is too optimistic and some variation from the constant value could be expected during the rupture propagation.

Another very important parameter is the expected rise time of the dislocation. The source time function could be a very complex function and is very difficult to be determined accurately at the present knowledge of fault rupture mechanism. The average slip velocity for many earthquakes is found to range between 1 m/s to 3 m/s. This results in a rise time between 1.1s to 3.5s for a dislocation of 3.5m. In the present investigation the whole range between 1s - 4s has been examined but we show only the results for a rise time of the order of 1.5s due to shortage of space.

The anelastic attenuation model used in the present investigation is presented in Table 3 while Table 4 depicts a simplified earth model in the area based in refraction investigations (Makris 1977).

Following the procedure presented above we try to synthesize the expected long period ground motion in Athens due to the expected Atalanti earthquake.

First we use eq.[13] to calculate the far field displacement spectra corresponding to each one subfault. During this calculation, the attenuation effect and the propagation effect of rupture within each segment are included. The first six modes were considered, and inverse FFT of the individual spectra gave the corresponding time-history surface wave motion for each segment.

Next, the individual time histories were filtered in the time domain, by means of an 8-pole Butterworth filter which was applied twice (in the forward and reverse directions) to compensate for phase changes. The time histories of the Love and Rayleigh waves from all the subfaults were summed taking in mind the time lags due to rupture and media propagation, and yielded the required surface wave ground motion at the site.

Fig. 8, shows the calculated surface wave ground motions for the city of Athens due to the expected Atalanti earthquake for two possible positions of rupture initiation. The maximum expected amplitudes were found to be about 16cm and 11cm for the two cases. the obtained higher amplitudes for case (a) can be explained as the result of the Doppler effect of the propagating rupture on the motions.

CONCLUSIONS

Various methods of generation of realistic input earthquake motions were introduced in this study.

Important ground motion parameters were determined on a consistent probabilistic basis, from a single risk index Po and the annual probability exceedance for peak RMS intensity.

Near field earthquake motions were generated by a semiempirical method in which simulated earthquake motions were used as Green's functions.

Surface wave motions were computed employing fault dislocation and normal mode theories.

ACKNOWLEDGEMENTS

The author wants to express his appreciation to K. Kudo for numerous discussions regarding the intricacies of long period wave motion synthesis and I. Muramatsu for sending important information concerning his method of synthesis. This project was partially supported by the Directorate Research and Development of the European Communities.

REFERENCES

Ben-Menahem, M., and Singh, A., (1981), Waves in elastic media, Springer Verlang, New York, p.877.

Boore, D., (1983), Stochastic simulation of high-frequency ground motions based on seismological models of the radiated spectra, Bull. Seism. Soc. Am. 73, 1865-1894.

Brun, J., (1970), Tectonic stress and the spectra of seismic shear waves from earthquakes, Jr. Geoph. res., 75, 4997-5009.

Comninakis, P., and Papazachos, B., (1986), A catalogue of earthquakes in Greece and the surrounding area for the period 1901-1985. Publication of the Geophysical Lab., University of Thessaloniki.

Dan, K., Tanaka, T., and Watanabe, T., (1986), Simulation and prediction of srong ground motion near earthquake fault, ORI Report 36-01.

Geller, R., (1978), Scaling relations for earthquake source parameters and magnitudes, Bull. Seism. Soc. Am., 65,

Hartzell, S., (1978), Earthquake aftershocks as Green's functions, Geoph. Res. Lett., 5, 1, 1-4.

Herrman, R.B., and Nuttli, O.W., (1975), Ground motion modelling at regional distances for earthquakes in a continental interior. I. Theory and Observations, Earthq. Eng. and Struct. Dyn., 4, 49-58.

Irikura, K., and Muramatsu, I., (1982), On a method to estimate strong motions of a large earthquake, Nat. Dis. Sci., 1-1, 29-43.

Kameda, H., and Nojima, N., (1988), Simulation of risk consistent earthquake motion, Earthq. Eng. str. Dyn., 16, 1007-1019.

Kameda, H., and Sugito, M., (1982), Microzonation and simulation of spatially correlated earthquake motions, Proc. 3rd Int. Microzonation Conf., Seattle, Vol.III, 1463-1474.

Kanamori, H., and Anderson, D.L., (1975), Theoretical basis of some empirical relations in seismology. Bull. Seism. Soc. Am., 65, 1073-1089.

Kiratzi, A., Karakaisis, G., Papadimitriou, E., and Papazachos, B.,C., (1985), Seismic source parameter relations for earthquakes in Greece. Pure Appl. Geophys., 123, 27-41.

Kudo, K., (1978), The contribution of Love waves to strong ground motions. Proc. 2nd Int. Conf. Microzonation, 765-776.

Kudo, K., (1980), A study of the contribution of surface waves to strong ground motions, Proc. 7th WCEE, Geosciences Aspects, II, 499-506.

Makris, J., and Vees, R., (1977), Crustal structures of the Aegean sea and the island of evia and Crete, Greece, obtained by refraction seismic experiments, Jr., Geoph., 42, 329-341.

Makropoulos K., and Burton, P., (1981), A catalogue of seismicity in Greece and adjacent area, Geophys. J. R. Astr. Soc., 65, 741-762.

Papazachos, B., (1980), Seismicity rates and long term earthquake prediction in the Aegean area. Quaterniones Geodaesiae, 3, 171-190.

Sato, R., (1979), Theoretical basis on relationships between focal parameters and earthquake magnitude, Jr. Phys. Earth, 27, 353-368.

Sugito, M., and Kameda, H., (1985), Prediction of nonstationary earthquake motions on rock surface, Proc. of JSCE, Vol.2, No.2, Oct., 1985.

Swanger, H.J., and Boor, D.M., (1978), Simulation of stromg motion displacements using surface wave model superposition. Bull. Seism. Soc. Amer., 68, 907-922.

Tanaka, T., Yoshizawa, S., Sakaue, M., and Osawa, Y., (1982), Estimation of acceleration characteristics of strong ground motion by synthesis of accelerogram obtained during a small earthquake, Bull. earthq. Res. Inst., 57, 561-579.

Tselentis, G-A., Stavrakakis, G., Makropoulos, K., Latousakis, J., and Drakopoulos, J., (1988). Seismic moments of earthquakes at the western Hellenic arc and their application to the seismic hazard of the area. Tectonophysics, 148, 73-82.

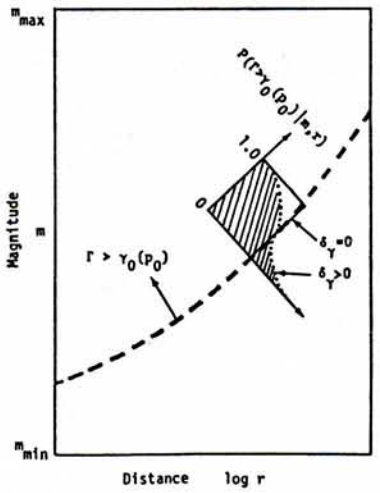

FIG.1: Conditional probability space of m,r for a specific value of Po (Kameda and Nojima 1988)

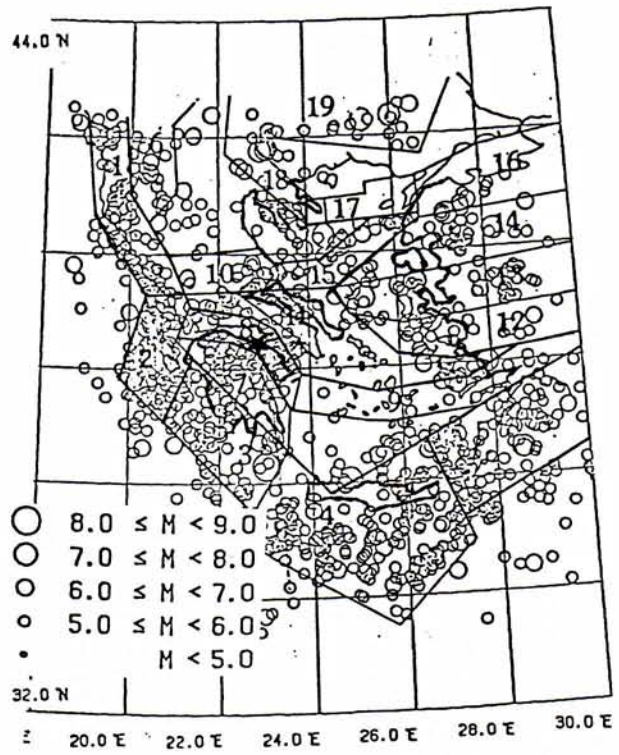

FIG.2: Seismic zones adopted in the analysis

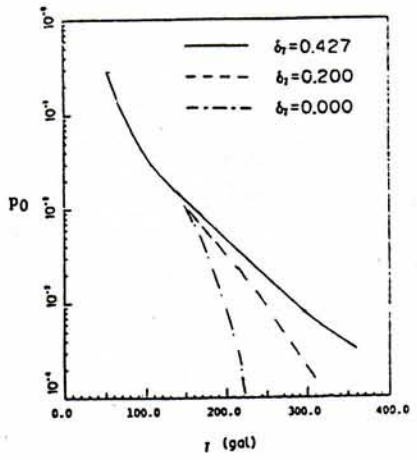

FIG.3: Hazard curve of Corinth

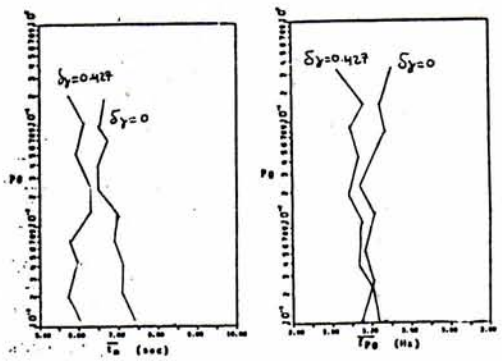

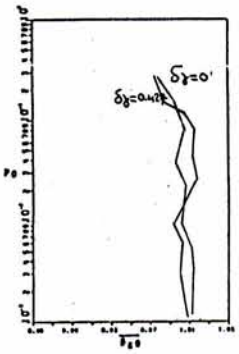

FIG.4: Conditional mean of t_m, f_{P0}, β_{P0}

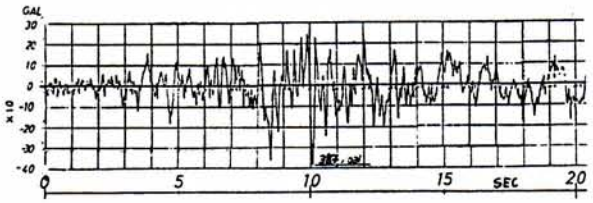

FIG.5: Example of simulated ground motion in Corinth.

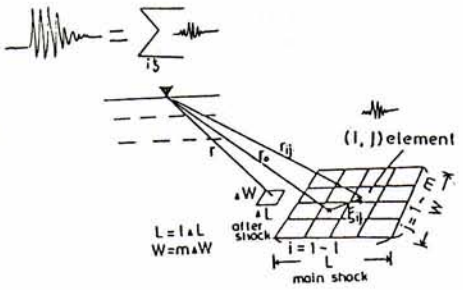

FIG.6: Description of the model used for the semi-empirical synthesis

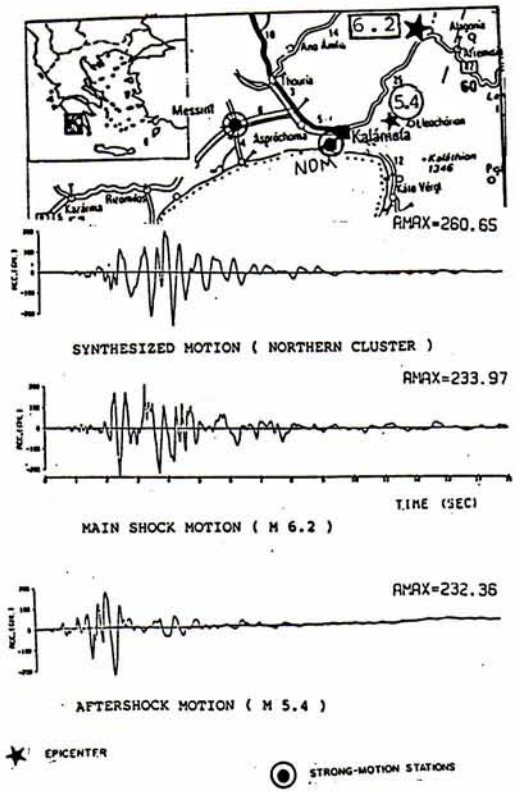

FIG.7: Comparison of the observed and synthesized motions at Kalamata. The aftershock used for the synthesis is also shown

Table I. The regression equations for ground motion model parameters

$$\log \gamma = 1{\cdot}950 + 0{\cdot}5371M - 1{\cdot}991\log(\Delta + 30{\cdot}0)$$
$$t_m = 19{\cdot}77 - 7{\cdot}35M + 0{\cdot}7196M^2 + 0{\cdot}0023(M-1)\Delta$$
$$f_{p0} = 4{\cdot}124 + (0{\cdot}0115 - 0{\cdot}0048M + 0{\cdot}000272M^2)\Delta + (-0{\cdot}7959 + 0{\cdot}2577M - 0{\cdot}01743M^2)10^{-4}\Delta^2$$
$$\beta_{s0} = -0{\cdot}2306 + 0{\cdot}2967M - 0{\cdot}0174M^2 + (-0{\cdot}0193 + 0{\cdot}0049M - 0{\cdot}0003M^2)\Delta$$
$$A_1 = \begin{cases} -11{\cdot}76 + 3{\cdot}187M - 0{\cdot}2158M^2; & M \leqslant 7{\cdot}5 \\ 0 \quad ; & M > 7{\cdot}5 \end{cases}$$
$$\log B_1 = -0{\cdot}02160 - 0{\cdot}5713\log(\Delta + 30)$$
$$f_p(t)_{\min} = 6{\cdot}78(10^{-0{\cdot}1M})$$

M; magnitude Δ; epicentral distance (km).

TABLE 3: Crustal models used

Vp	Vs	P	h
4.0	2.3	2.4	1.1
5.5	3.2	2.7	5.5
6.0	3.9	2.8	21.8
7.6	4.3	3.0	66.0

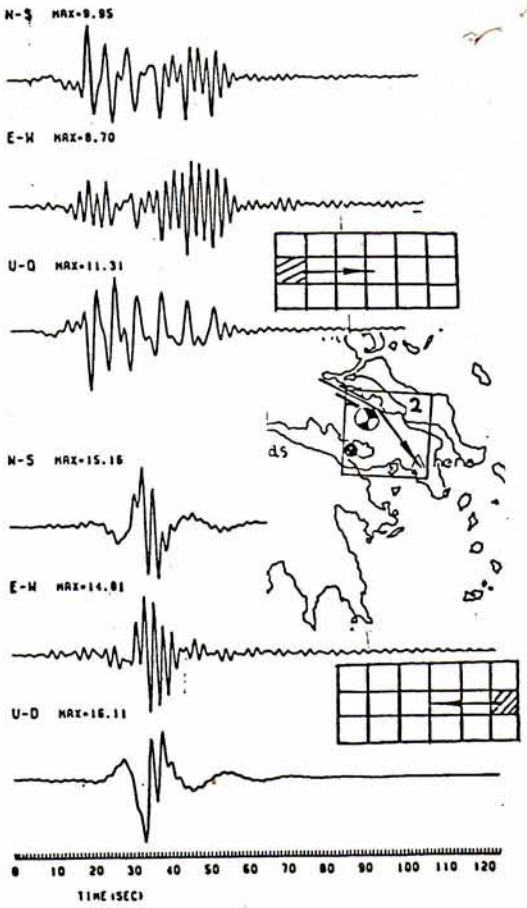

FIG.8: Displacements (long period) from the expected Atalanti earthquake at Athens

TABLE 2. Source parameters for the 1986 Kalamata earthquake.

Characteristics		Main Shock	Aftershock
Latitude		37.110° N	37.040° N
Longitude		22.140° E	22.130° E
Focal depth		6.2 km	4.0 km
Magnitude	(Ms)	6.2	5.4
Fault length	(L)	14. 7 km	4.7. 2.3 km
Fault width	(W)	14 km	4.7 km
Dislocation	(D)	15. 30 cm	5. 10 cm
Seismic moment	(Mo)	8.8×10^{24} dyne.cm	3.3×10^{23} dyne.cm
Effective stress	(σ_e)	30 bar	30 bar
Corner frequency	($\omega_c/2\pi$)	0.277 Hz	0.832 Hz
Distance	(r)	11.1 km	4.4 km
		Common Parameters	
Rigidity	(μ)	3×10^{11} dyne/cm^2	
Shear wave velocity	(β)	3 km/sec	
Density	(ρ)	3.3 g/cm^3	
Quality factor	(Q)	200	

TABLE 4

Period (sec)	attenuation parameter (Km^{-1}) Foundamental mode	Higher modes
1.0	0.01000	0.00050
2.0	0.01000	0.00050
2.5	0.00500	0.00050
5.0	0.00070	0.00050
10.0	0.00040	0.00020
15.0	0.00025	0.00000
20.0	0.00015	-
60.0	0.00015	-
100.0	0.00000	-